ACOUSTIC INTERROGATION AND IMAGING OF COMPLEX SUB-SURFACE SEABED BURIED DEBRIS

J.Y.Guigné Kraken Robotics, Mount Pearl, Newfoundland and Labrador, Canada
R.Laidley Kraken Robotics, Mount Pearl, Newfoundland and Labrador, Canada

1 INTRODUCTION

Three-dimensional (3-D) investigations of the shallow sub-seabed for identifying and characterizing geohazards and stratigraphy require specular and non-specular returns with spatial accuracies exceeding those of current conventional seismic surveys (i.e., towed streamer-based methods). Advanced acoustic imaging enables improved correlations between acoustic and geotechnical properties of near-surface soils. To effectively image geohazards (e.g., boulders, pipes, etc.) and stratigraphic characteristics (e.g., small-scale sand/shale lenses) requires retention of the entire signal energy distributions, principally the diffuse diffracted signals and the dominating reflective energy and location calibrations. This is accomplished by sub-seabed interrogation through a stationary transmitter and receiver array holding a spatial centimetre-spaced network through a horizontal imaging dimension of 14 metres.

The study area for the seismic focusing innovation was the Gulf of Mexico, where a sub-bottom/below mudline (BML) survey of 63 Acoustic Corer (AC) scans (see Figure 1) was investigated to determine the extent, expanse, orientation and characteristics of lost conductor pipes. The survey area investigated was 205m (673ft) x 60m (197ft). Each acoustic core result provided a 14m (46ft) diameter volumetric image of the sub-bottom down to a penetration depth of approximately 60m (200ft).

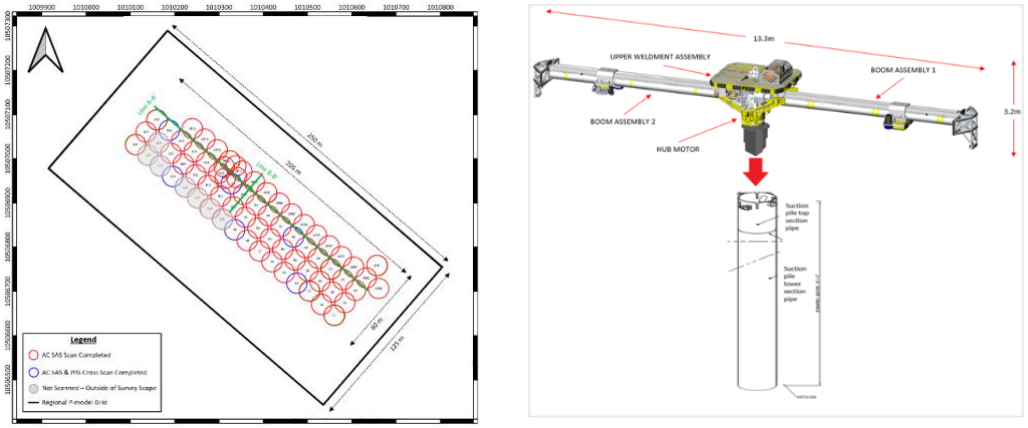

Figure 1: Right - Sixty-three (63) acoustic core survey area layout; left - each collected off of a suction pile set-up

2 ACOUSTIC CORER (AC)

The approach called “Acoustic Sub-seabed Interrogation” (ASI) was first introduced by Guigné in 1986 at the University of Bath[1]. This technique was designed to acquire the backscattering response of discrete targets within the sub-seabed using a dense data acquisition grid [2, 3]. The first ASI design was an experimental model that involved a platform that supported 16 planar sparker transmitters in an octagonal polyethylene framework held by an aluminum outer structure [4]. A 12m-long (39ft) rotating boom at the apex of the instrument provided support to 12 equally spaced calibrated hydrophones. The 12 receivers were rotated during data collection and aligned with four transmitters to form a transmitting-receiving row called a “beam,” delivering four linear “beams” of data. The resulting data was processed and rendered into a 3-D volumetric image with a minimum 10m diameter (33ft) and a sub-seabed penetration depth of over 10m (33ft). This stationary acoustic acquisition

"lens" provided the first "Acoustic Core" solution involving a 3-D determination of geophysical parameters of the subsurface while maintaining signal coherence between repeated echoes.

Figure 2:Transmit/receive package

2.1 Hardware Description

The concept has been further developed since 2006 [5,6]. The apparatus now consists of three sonar heads attached to each arm of a 12m (39ft) boom held and rotating off tripod legs (see Figure 2). This boom turns 180°, creating a 360° acoustic core product 14m (46ft) in diameter down to a depth of 60m (200ft). The sonar heads contain three collocated acoustic sensors: an HF chirp (operating across 4.5–12.5kHz), an LF chirp (operating across 1.5–6.5kHz) and a Parametric source (using a secondary frequency (f_s) of 8kHz).

The Parametric source has a narrower acoustic propagation pattern than the HF chirp, providing more detailed, crisper imagery of the features. Collocated confidence is derived with the HF chirp, and critical imagery elements are confirmed in target-picking. The survey area comprised soft, low load-bearing sediment, challenging most seabed-deployed survey equipment, including the standard AC configuration. To overcome this, a 15.8m (52ft) long suction pile was used as the deployment method instead (Figure 1) [7]. Using a vessel crane, a suction pile was positioned at each AC survey location to a depth of approximately 12.8m (42ft).

2.2 Theoretical Background

The acoustic wave equation governs the modelling and imaging of targets under the assumption of a constant-density medium. Every target is modelled as discrete, compactly supported perturbations of a global background sound speed function defined in the 3-D Cartesian space R^3. The full wave speed function is decomposed as

$$c(x) = c_o(x) + \Delta c(x)$$

where c_o represents a smooth background model and Δc represents any diffractions or scatterers. The acoustic wave equation in the frequency domain (Helmholtz equation) has the form:

$$\left(\nabla^2 - {\omega^2}/{c^2}\right) u(x, x_s, \omega) = \delta(x - x_s)$$

where ω is the angular frequency, u is the full wavefield and δ is the dirac delta function.
Following the Born geometric optics approximations, the scattered wavefield can be expressed in the frequency domain as:

$$u(x, x_s, \omega) = -\omega^2 \int_\Omega u_i^0(\xi, x_s) u_i^0(\xi, x) e^{i\omega(\tau(\xi, x_s) + \tau(\xi, x))} \Delta^2 s(\xi) d\xi$$

Using the generalized back-projection operator from Beylkin [8] the imaging operator is defined as

$$R^* u_s(x) = \int_{\delta\Omega} u_s\big(\xi, x_s, \phi(x, x_s, \xi)\big) w(x, x_s, \xi) d\,\xi$$

This imaging operator is recognized as a weighted diffraction summation (integration) over the aperture of the recorded data. Explicitly, the summation is carried out over the diffraction curve defined by φ and scaled by w.

3 DATA ACQUISITION AND PROCESSING

3.1 Geotechnical Information of the Survey Area

The survey area [9] is largely comprised of clay, with the top 18–21m (59–69ft) suggestive of mass flow deposits. As a result, this material is highly variable, with undrained shear strengths approaching zero near the mudline (i.e., seabed surface), increasing to about 26.3kPa around 23m (75ft) BML. However, more rigid material could still be encountered at shallower depths depending on whether blocky material exists within the mass transport deposits. Below 23m (75ft), the soil is less variable but under-consolidated with undrained shear strengths ranging from 28.7–33.5kPa between 24–61m (78–200ft) BML. These shear strengths are nearly three times lower than those typically encountered in other regions of the Gulf of Mexico.

3.2 Data Acquisition and Processing

The uppermost seabed (7.3m (24ft) BML) is characterized by soft sediments with low shear strength (<10kPa). These conditions required close stability monitoring during the deployment of the AC using a crane. Immediately after landing and transferring the weight of the AC to the seabed, the AC's depth, altitude, pitch and roll were recorded, and stability tests were performed. The AC was rotated after determining that the system was stable in static mode. The acoustic payloads moved out of the booms to their baseline positions while continually monitoring pitch, roll and altitude via the onboard sensors on the main frame and acoustic payloads.

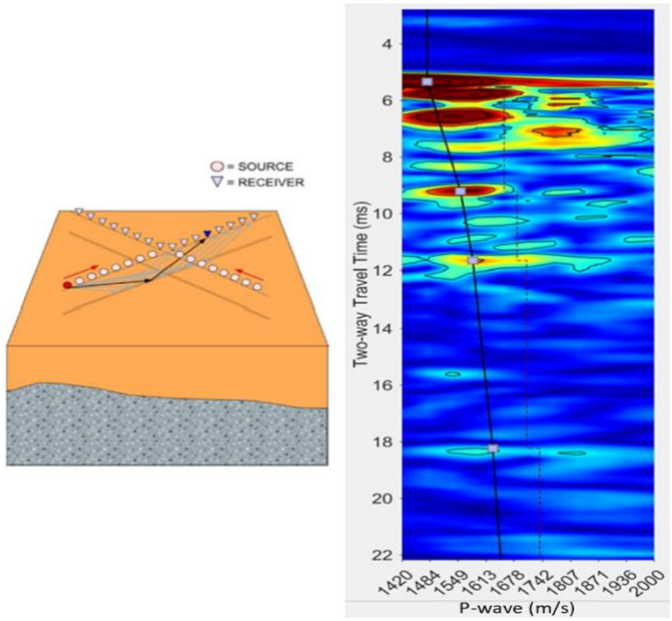

Figure 3: Left: JYG-cross data acquisition configuration; Right: Semblance analysis (i.e., velocity profiles) for p-model creation.

3.2.1 JYG-Cross and Regional P-model Generation

The JYG-Cross[10,11] technique resembles a high-precision seismic line that folds the data to accentuate sub-seabed stratigraphy, similar to multichannel marine seismology.

It collects approximately 5000 data points along two pseudo-orthogonal lines using the LF chirp at an interval spacing of 10cm (4in) (See Figure 3).

These data sets are used to perform 2-D semblance analysis to derive soil velocity profiles (V_{rms}) and subsequent velocity models. Velocity models (p-models) are 3-D volumes generated to provide the coordinates and soil velocities of the points that will be imaged.

In this study, JYG-Cross data was collected at six scan locations throughout the survey area (Figure 1) and six velocity profiles (V_{rms}) were formed. These V_{rms} profiles were then used in a gridded interpolation to generate a regional velocity The model covered the entire survey area and was 250m

(820ft) by 125m (410ft) (Figure 1). The utilized X-Y-Z grid had an interval spacing of 10cm by 10cm for the X-Y plane and 0.02 ms for the Z-interval. Figure 4 shows a cross-section of the RMS velocity model created using the six velocity profiles. All 63 AC volumes were processed through standard seismic processing steps. Static corrections were applied (refer to Figure 5).

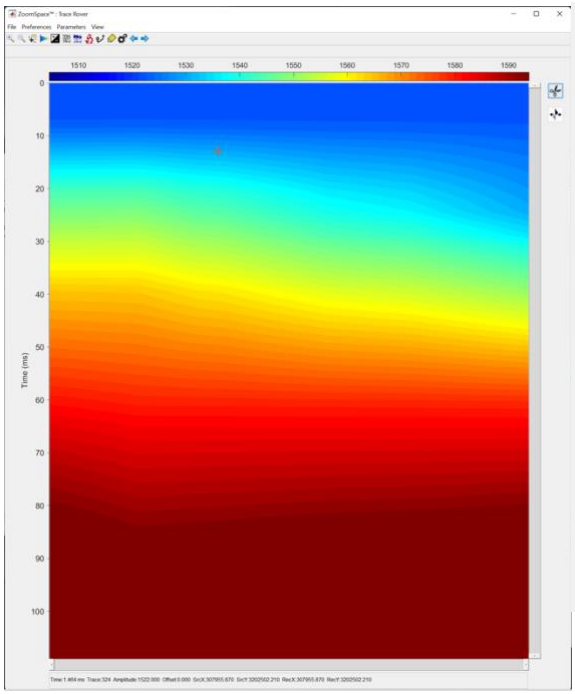

Figure 4: Regional RMS velocity model cross-section

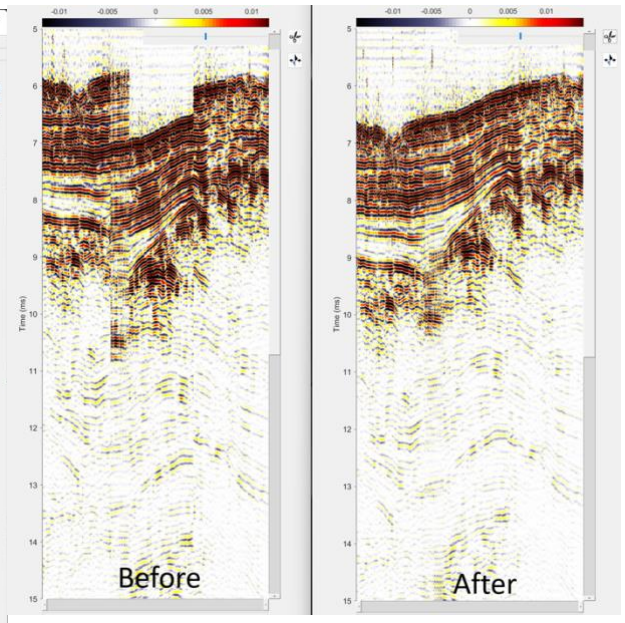

Figure 5: Left: Before static correction and Right: after static correction

3.2.2 Imaging and Horizon Picking

The individual pre-processed volumes were merged and migrated into a single cohesive volume statically corrected to the same reference datum (Figure 5 to Figure 7). This enabled a more unified identification and interpretation of the conductors. The detailed processing flow is shown in Figure 8.

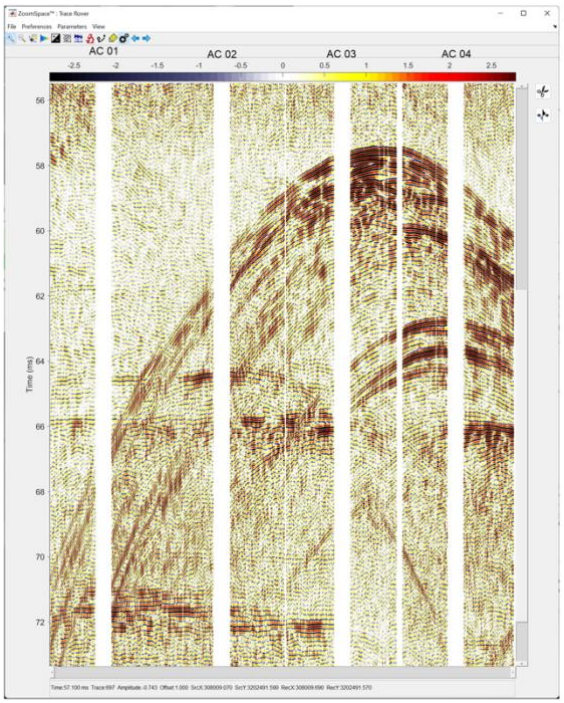

Figure 6: To the right- After static correction showing the acoustic response from the conductors at depth

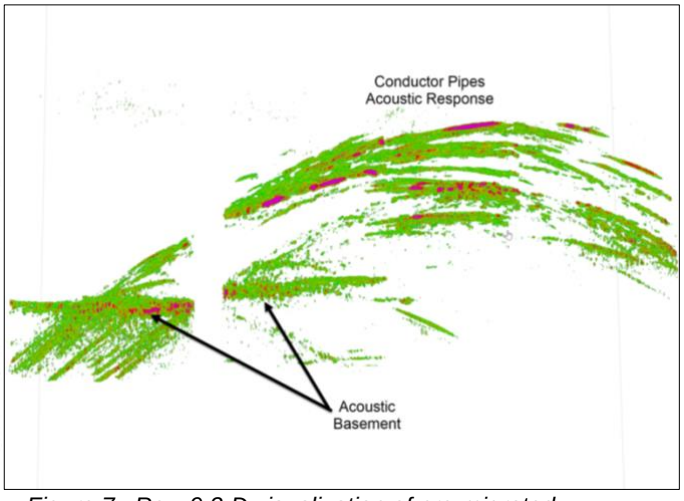

Figure 7: Row 9 3-D visualization of pre-migrated acoustic data

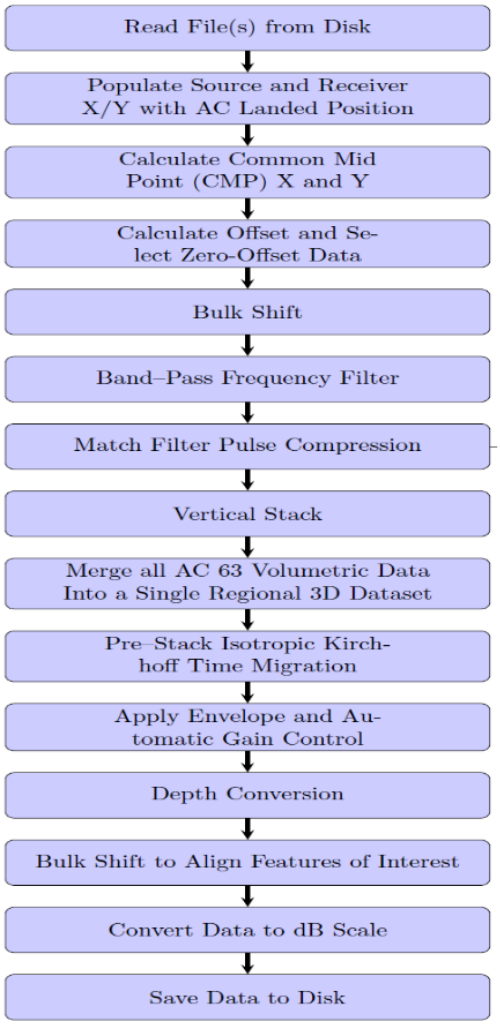

The post-processed migrated volume was analyzed using OpendTect software to interpret and pick the seabed, conductors, and basement horizons. Initial interpretation began with the seabed, where a grid was generated using the inline/crossline data. Each grid line was tracked along the seabed horizon, appearing as a continuous bright reflector within the data (Figure 9). A similar approach was used to construct a series of grid lines representing the basement surface. Once completed, a gridding technique was applied using an inverse distance weighted algorithm. The grids were filtered and smoothed using an average-type weighting scheme, and the 3-D horizon surfaces were created (Figure 10).

The conductors were evaluated in a cross-section (inline) view, tracking the bulls-eye response of each feature along the unified dataset (Figure 11). A location point was marked for every visible conductor at each inline interval. This procedure was repeated throughout the migrated volume until the full extent of each conductor had been identified. A total of 18 conductors were interpreted, comprising a digitization of approximately 40–50 location points per conductor. The 18 conductors and the inferred seabed and basement horizons were then imported into EIVA's NaviModel visualization software for further analysis (**Error! Reference source not found.**).

Figure 8: Data processing workflow

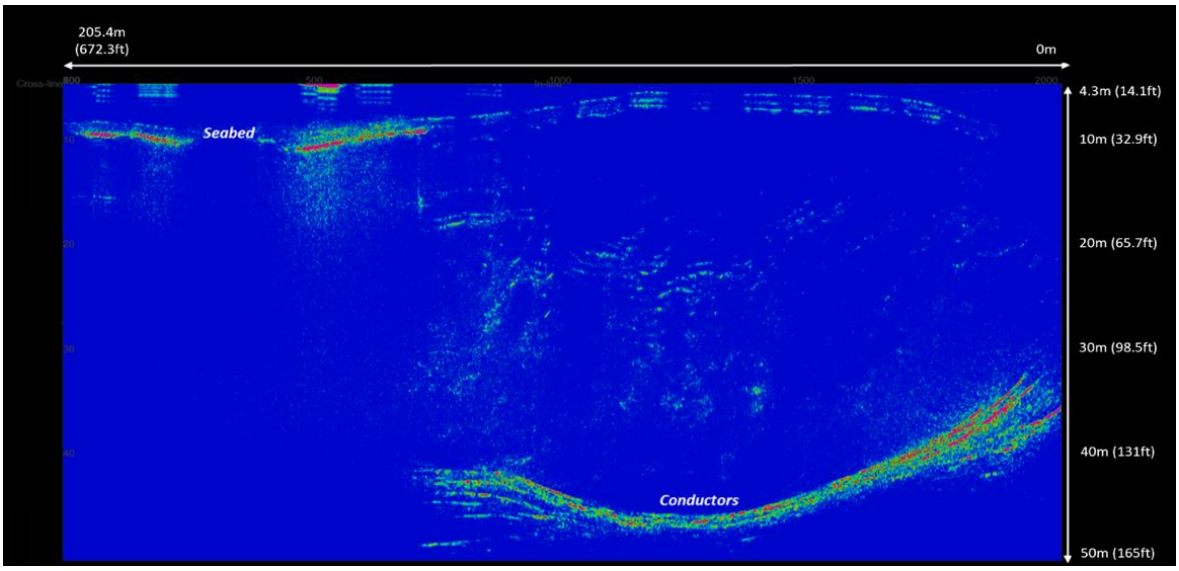

Figure 9: Conductors exhibited as continuous bright reflectors within the data

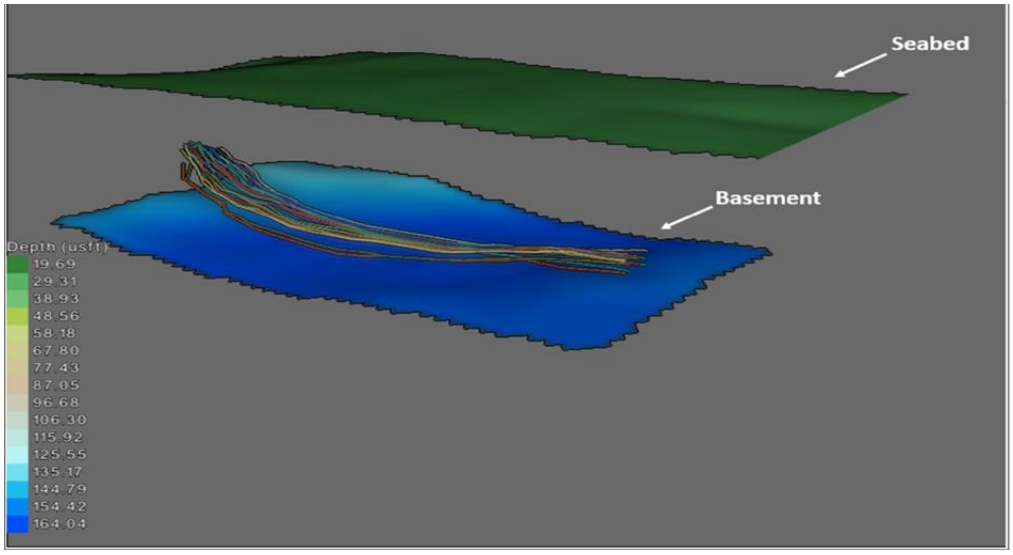

Figure 10: The 18 conductors and the inferred seabed and basement horizons are illustrated

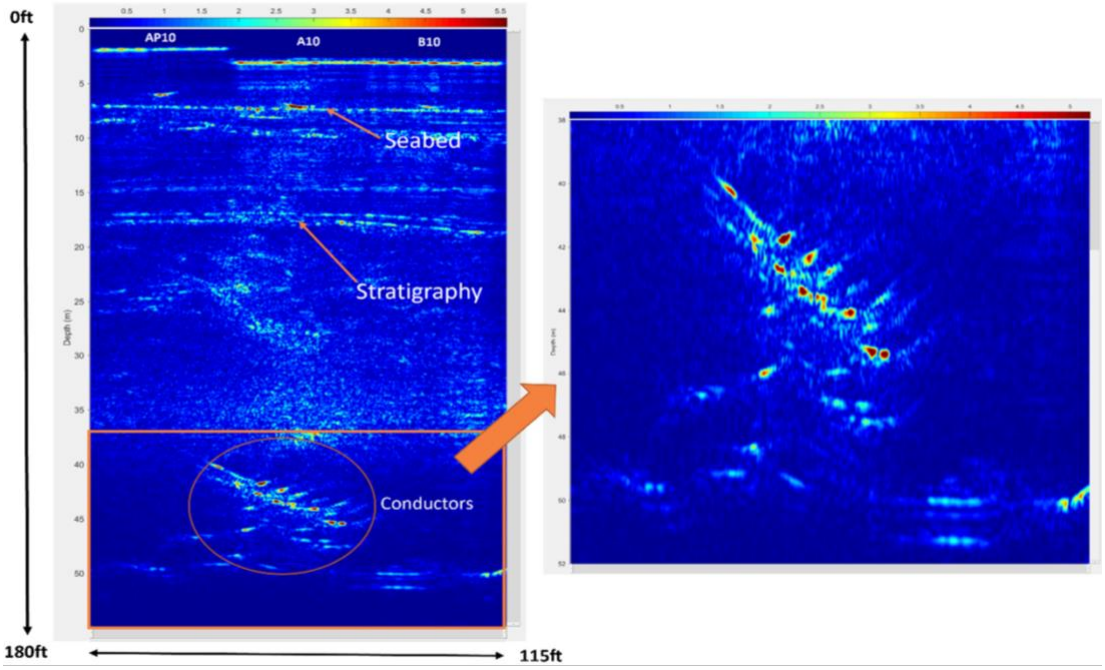

Figure 11: The conductors were evaluated in a cross-section (inline) view, to the left tracking the bulls-eye response of each feature along the unified dataset

4 INTERPRETATION

The AC data sets accurately captured not only the specular returning sedimentary signals but, more importantly, the non-specular returns of the conductors. They delivered a volumetric image of the conductors' presence, characterizing their depth, shape, size and form. A continuous traverse from NW to SE was observed (Figure 12). In the upper region of the sub-seabed, the upper 18m (59ft), the composition is characterized by an unconsolidated chaotic nature, sometimes blocky, associated with a flow event. Clay-based linear diffractors are present within this region's weak, non-cohesive sediment matrix. Close examination of the reflecting responses of the clay strata supports an assignment of undrained shear strengths associated with a very soft fluid state at the mudline (near 0kPa) to soft denser clay in the strata (12–25kPa).

The conductors appear as a bundle primarily in Lines AP and A (Figure 1) running NW-SE, where an apparent, abrupt termination is observed (Figure 9). These conductors are found at depths between 27.7–48.1m (91–158ft), with the greatest concentration between 39.6–47.2m (130–155ft). The shallowest conductor appears at 27.7m (91ft), trending downwards from the toppled jacket (Figure 10). The cross-sectional analysis of the conductor bundle positively identified 18 individual conductors (Figures 10, 11 and 12). By migrating all the cores together, the spatial resolution was improved. This provided additional clarity on the continuity of the conductors and enabled discrimination with a high degree of confidence.

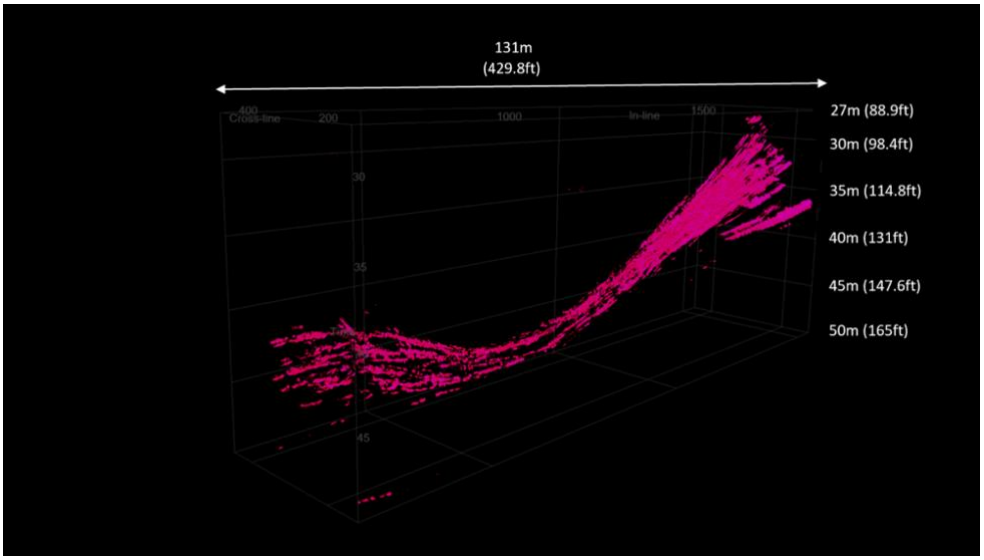

Figure12: The cross-sectional analysis of the conductor bundle identified 18 individual conductors

5 CONCLUSIONS

Fusing in a cellular manner rather than as mosaic data sets resulted in augmented clarity over a large volume of the subseabed. This enabled a higher level of detail in the distribution of geological and geotechnical properties, including the nature of geohazards and stratigraphy. This is evident by how the buried conductors were captured and delineated for the first time. This methodology can augment the decommission of buried debris fields of abandoned oil and gas sites.

6 ACKNOWLEDGEMENTS

The authors would like to thank the offshore Geoscientists and Operations team of Kraken Robotics for collecting and handling these data sets; special mention is given to Dr. Maria Kotsi, Stephanie Abbott and Cevdet Anil Kilic. They also thank Dillon Hoffmann and Dr. Kevin Kennelley of Couvillion Group for their support throughout the Gulf of Mexico campaign.

7 REFERENCES

1. J.Y. Guigné, The Concept, Design and Experimental Evaluation of Acoustic Sub-seabed Interrogation. Ph.D. thesis, University of Bath, Bath, UK (1986)

2. J.I. Clark and J.Y. Guigné, Marine Geotechnical Engineering in Canada. Canadian Geotechnical Journal. 25 (2), 179-198. (1985)

3. J.Y. Guigné and V.H.Chin, Acoustic Imaging of an Inhomogeneous Sediment Matrix. Marine Geophysical Researchers. 11, 301-317 (1989)

4. S.T. Inkpen, J. English, C.J. Pike, J.Y. Guigné, J. Guzzwell, P. Hunt and K. Tuff, A Three-dimensional Acoustic Site Surveying Probe. OTC 91, 23rd Annual Offshore Technology Conf Procs. Vol 1, Ppr OTC 6559, pp. 525-535. (1991)

5. J.Y. Guigné, Acoustic Interrogations of Complex Seabeds. D.Sc. Thesis. University of Bath, Bath, UK. (2014)

6. J.Y. Guigné and P. Blondel, Acoustic Interrogations of Complex Seabeds. Springer Briefs, Heidelberg (2017)

7. R. Laidley, J.Y.Guigné, M.Kotsi, S.Abott, C. A. Kilic, D.Hoffmann, and K. Kennelley, Imaging Conductor Pipes in the Gulf of Mexico Using 3-D High-Resolution Seismic Data: Containing one of the Largest Oil Spills in US History Oceans Gulf Coast (2023)

8. G. Beylkin, Imaging of Discontinuities in the Inverse Scattering Problem by Inversion of a Causal Generalized Radon Transform. J. Math. Phys. 26 (1) (1985)

9. S. Abbott, M. Kotsi, R. Laidley, C. A. Kilic, and J. Y. Guigné, Merging individual Acoustic Corer data sets into a unified volume to optimize the identification and interpretation of geohazards, obstructions and stratigraphy: Case studies from the Baltic Sea and Gulf of Mexico" Society for Underwater Technology, 9th International Offshore Site Investigation and Geotechnics Conference: Innovative Geotechnologies for Energy Transition, (2023)

10. D. Hoffmann, K.J. Kennelley, J.Y. Guigne and R. Laidley A Geotechnical Acoustic Survey to Address Well Abandonment Options for A Toppled Offshore Platform, OTC (2024)

11. J.Y. Guigné, J.K Welford and I.R. McDermott, Volumetric, Multi-fold Acoustic Interrogations of Complex Sub-seabeds. Near Surface, EAGE – Zurich (2010)

12. J.Y. Guigné, J.K. Welford, A. Gogacz and C. Clements, US Patent Application- Method for Accentuating Specular and Non-Specular Seismic Events from within Shallow Subsurface Rock Formations (2012)